ACS APPLIED MATERIALS & INTERFACES

Research Article

www.acsami.org

Micropatterned Azopolymer Surfaces Modulate Cell Mechanics and Cytoskeleton Structure

Carmela Rianna,[†,§] Maurizio Ventre,[†,‡] Silvia Cavalli,[§] Manfred Radmacher,[∥] and Paolo A. Netti*[,†,‡,§]

[†]Department of Chemical, Materials and Industrial Production Engineering and [‡]Interdisciplinary Research Center on Biomaterials, University of Naples Federico II, Piazzale Tecchio 80, 80125 Naples, Italy

[§]Center for Advanced Biomaterials for Healthcare IIT@CRIB, Istituto Italiano di Tecnologia, Largo Barsanti e Matteucci 53, 80125 Naples, Italy

[∥]Institute of Biophysics, University of Bremen, Otto-Hahn Allee, D-28359 Bremen, Germany

ABSTRACT: Physical and chemical characteristics of materials are important regulators of cell behavior. In particular, cell elasticity is a fundamental parameter that reflects the state of a cell. Surface topography finely modulates cell fate and function via adhesion mediated signaling and cytoskeleton generated forces. However, how topographies alter cell mechanics is still unclear. In this work we have analyzed the mechanical properties of peripheral and nuclear regions of NIH-3T3 cells on azopolymer substrates with different topographic patterns. Micrometer scale patterns in the form of parallel ridges or square lattices of surface elevations were encoded on light responsive azopolymer films by means of contactless optical methods. Cell mechanics was investigated by atomic force microscopy (AFM). Cells and consequently the cell cytoskeleton were oriented along the linear patterns affecting cytoskeletal structures, e.g., formation of actin stress fibers. Our data demonstrate that topographic substrate patterns are recognized by cells and mechanical information is transferred by the cytoskeleton. Furthermore, cytoskeleton generated forces deform the nucleus, changing its morphology that appears to be related to different mechanical properties in the nuclear region.

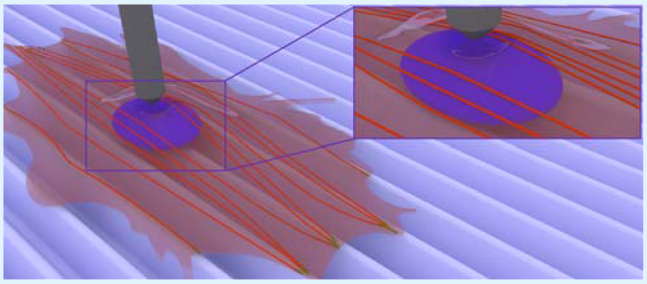

KEYWORDS: *topographic patterns, azopolymers, cell mechanics, AFM, cytoskeleton, cell nuclei*

1. INTRODUCTION

Understanding the interactions between cells and the extracellular environment to create adequate conditions to elicit and sustain specific cellular functions is one of the critical aspects in tissue engineering and regenerative medicine.[1,2] Within this context, the presence of adhesive ligands plays a crucial role. In particular, natural extracellular matrix (ECM) regulates via mechanical,[3] biochemical,[4] or topographical cues,[5] many cellular processes eventually determining the cellular behavior. Biomaterial surfaces with engineered physical/chemical features have been developed in recent years in order to control and guide cell fate.[6−8] Even though the biochemical mechanisms regulating the transduction of adhesive signals into a biological response are not thoroughly understood, there is growing evidence that focal adhesion (FA) mediated signaling and cytoskeleton-generated forces play a fundamental role.[9] Cell adhesion and cytoskeletal assembly are the major determinants of the cell mechanical behavior. Indeed, cell elasticity can be largely influenced by the cell−substrate interface interactions. Moreover, in recent years, cell mechanics investigation has proven to be a promising tool for applications in the field of regenerative medicine, in which cell mechanical properties can be quantitative markers, monitoring the regulation of cell differentiation,[10−12] or within clinical and medical contexts such as in cancer diagnostics.[13,14] Cell mechanics can be evaluated with several methods, such as micropipet aspiration,[15] optical tweezers,[16] magnetic twisting cytometry,[17] or atomic force microscopy (AFM).[18] Among these, AFM is the most widely used technique for adherent cells, allowing both topographical imaging and measuring mechanical properties of heterogeneous living samples, such as cells. By obtaining force−distance AFM curves, cell elastic properties can be measured in terms of elastic or Young's modulus. In order to understand the interaction between ECM signals and cell mechanics, several studies have been performed. For example, it has been shown that cell spreading and stiffness directly depend on mechanical properties of the underlying materials.[19,20] Even though topographic cues proved to be a powerful tool to control different aspects of the cell behavior, there are only few reports concerning the effects of topographies on cell mechanics. In particular, submicrometer scale topographic patterns were reported to alter the FA−cytoskeleton−nuclear shape axis and changes in nuclear morphology might have a direct impact on gene expression.[21,22]

However, the possible interplays between topography and nuclear mechanics have not been clarified yet.

Received: July 23, 2015
Accepted: September 15, 2015
Published: September 15, 2015

DOI: 10.1021/acsami.5b06693
ACS Appl. Mater. Interfaces 2015, 7, 21503−21510

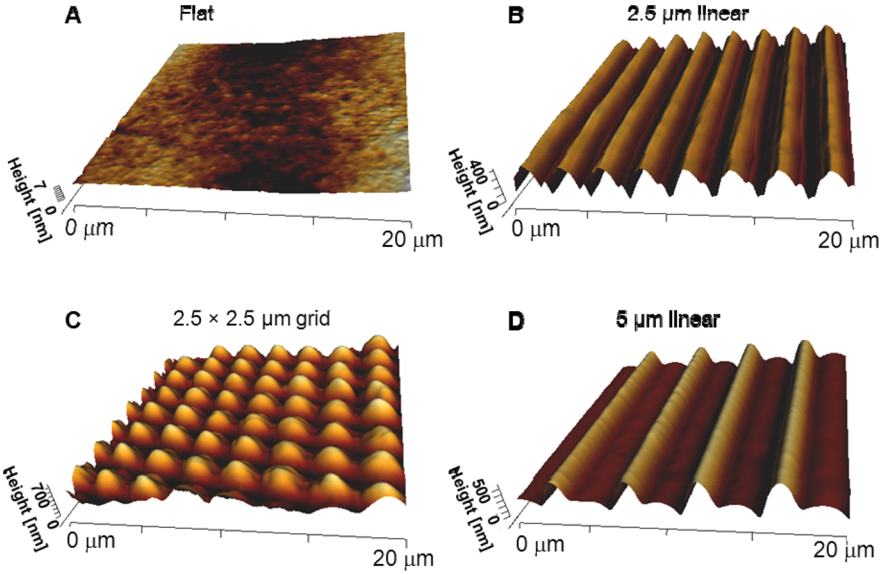

Figure 1. Three-dimensional height AFM images of (A) flat spin coated pDR1m on bare glass; (B) 2.5 μm pitch linear pattern on pDR1m realized by use of the Lloyd's mirror technique; (C) 2.5 × 2.5 μm grid pattern obtained by overlapping two orthogonal patterns with the Lloyd's mirror technique; (D) 5 μm pitch linear pattern embossed on pDR1m with the single laser beam technique. Image size is 20 × 20 μm.

In this study we investigated the influence of microgrooved patterns on the local elasticity of fibroblast cells, their cytoskeletal organization, and the shape of cell nuclei. Micropatterns were fabricated using azopolymers and cell mechanics was investigated with AFM. Topographies were encoded on the material surfaces in a contactless manner by means of either structured light or with a laser beam. AFM force mappings were performed in order to draw out the dependence of the local elastic modulus on cell height. This allowed us to gain information on cell stiffness in selected cell regions and, most importantly, on how cell stiffness was modulated by the underlying topography.

2. MATERIALS AND METHODS

2.1. General Materials. Poly-Disperse Red 1-methacrylate (pDR1m), TRITC-phalloidin, Triton X-100, and Dulbecco's modified Eagle's medium (DMEM) were purchased from Sigma; Alexa Fluor 488 conjugated goat antimouse antibody and To-Pro3 were purchased from Molecular Probes (Life Technologies), antivinculin monoclonal antibody was purchased from Chemicon (EMD Millipore); circular cover glasses were purchased from Thermo Scientific. Chloroform and other solvents were purchased from Romil.

2.2. Substrate Preparation. pDR1m was dissolved in chloroform at a 5% w/v concentration. The solution was spun over 12 mm diameter cover glasses by using a spin coater at 1500 rpm (Laurell Technologies Co.). Different patterns were inscribed on azopolymer films by using a Lloyd's mirror setup, as described elsewhere.[23,24] Briefly, an interference pattern of light was realized by reflecting the horizontally polarized light source (442 nm He−Cd laser) on a mirror. The spin coated pDR1m glass was fixed to the edge of the mirror, forming a right angle with the mirror surface, and the interference pattern of light was able to induce a relief grating on the sample surface. Pattern periodicity was controlled by adjusting the angle between the incident beam and the mirror. By using this technique, 2.5 μm pitch linear patterns were realized, and then 2.5 × 2.5 μm grid structures were obtained repeating the process twice after rotating the sample by 90°. Exposure time was 10 min for each inscription. The 488 nm argon laser line was employed to produce 5 μm pitch linear patterns on pDR1m with the single laser-induced patterning technique.[25,26] In the following, substrates will be referred to as 2.5 or 5 μm linear patterns and 2.5 × 2.5 μm grid pattern. Flat pDR1m spin coated glasses were used as control samples. Additional controls were polystyrene Petri dishes (35 mm, Corning) and bare cover glass slides.

2.3. Cell Culture. NIH-3T3 fibroblasts were seeded on the substrates directly and without any further treatment, at an initial density of 2000 cells/cm^2. Cells were cultivated in low glucose DMEM, supplemented with 10% FBS (fetal bovine serum) and incubated at 37 °C in a humidified atmosphere of 95% air and 5% CO_2. pDR1m substrates were sterilized under UV light for 30 min, and then cells were seeded on them 48 h prior to AFM measurements.

2.4. AFM Experiments. An MFP3D AFM (Asylum Research) was used to measure mechanical properties of living cells. An optical microscope was combined with the AFM to position AFM tips on a particular sample location. Soft cantilevers (MLCT, nominal spring constant 0.01 N/m, Bruker) were used to investigate cell mechanical properties. Petri dishes were fixed to an aluminum holder with vacuum grease and mounted on the AFM stage with two magnets; all the setup was enclosed in a home-built poly(methyl methacrylate) (PMMA) box in order to maintain 5% CO_2. To acquire AFM images of patterned and flat substrates, JPK NanoWizard II (JPK Instruments) was used with MLCT tips, in contact mode and in air at room temperature.

2.5. AFM Data Acquisition. AFM images were acquired by setting the equipment in contact mode at a scan rate of 1 line per second. Before force mapping, the spring constant of each cantilever was first calibrated by the thermal tune method.[27] Force curves were typically recorded at a scan rate of 1 Hz at 4 μm z travel range, corresponding to a maximum typical loading rate of up to 6 nN/s and a maximum force of 0.7 nN. In detail, the trigger threshold for cantilever deflection was set at 100 or 150 nm, so that the force was controlled during each indentation. Typically, 400 force curves were measured over a cell area of 30 × 30 μm.

2.6. AFM Data Analysis. Mechanical properties of cells, in terms of Young's modulus (E) values, were calculated from each force curve within a force map. Evaluation was performed with the data analysis package IGOR (Wavemetrics). The Hertzian model was used to calculate Young's modulus for every force curve; therefore 400 values were generated for each force map.[28,29] Statistical analysis on Young's modulus distributions was performed with the Kruskal−Wallis test in Matlab.

2.7. Cell Staining. For confocal image acquisitions, NIH-3T3 fibroblasts were fixed after 48 h from cell seeding with 4% paraformaldehyde for 20 min and then permeabilized with 0.1% Triton X-100 in PBS 1× for 3 min. Actin filaments were stained with TRITC-phalloidin. Samples were incubated for 30 min at room

DOI: 10.1021/acsami.5b06693
ACS Appl. Mater. Interfaces 2015, 7, 21503−21510

temperature in the phalloidin solution (dilution 1:200). For focal adhesion (FA) staining, cells were immersed in an antivinculin monoclonal antibody solution (dilution 1:200) for 2 h and labeled with Alexa Fluor 488 conjugated goat antimouse antibody (dilution 1:1000) for 30 min. Finally, cells were incubated for 15 min at 37 °C in a To-Pro3 solution (dilution 5:1000) to stain cell nuclei. A Leica TCS SP5 confocal microscope (Leica Microsystems) was used to collect fluorescent images of cells; the laser lines used were 488 (vinculin), 543 (actin), and 633 nm (nuclei). Emissions were collected in the 500−530, 560−610, and 650−750 nm ranges, respectively. Fiji software was used to measure the cell nuclei aspect ratio (A/R) and volume from three-dimensional *z*-stacks.[30] In detail, we assumed an ellipsoidal shape for cell nuclei; therefore the volume was measured with the formula $V = 4/3\pi abc$, in which *a*, *b*, and *c* are the main semiaxes. The semiaxes of the equatorial plane were calculated with Fiji by using the analyze particle command performed on the projected image of the *z*-stack. The semiheight *c* was calculated with the orthogonal views tool of Fiji.

3. RESULTS AND DISCUSSION

Surface topography can affect FA formation and cytoskeleton assembly up to nuclear shape.[21] In this work, topographic patterns were encoded on light responsive pDR1m substrates, through two different optical methods: Lloyd's mirror and single laser patterning technique, respectively. These methods were effective in transferring long-range patterns with micrometer scale features on pDR1m (Figure 1).

The Lloyd's mirror technique allows quick and easy encoding of topographic features, but with rather limited geometrical characteristics. Conversely, with the laser beam technique, patterns displaying different shapes of different length scales can be created in a few minutes. Cells can be cultured on azopolymer substrates without any additional functionalization.[31] The geometrical features of the patterns we produced were inspired by our previous experiences on cell−topography interactions demonstrating that micrometer- and submicrometer-scale patterns can alter cell elongation, orientation, and nuclear shape.[21,31,32] We hypothesized that pattern mediated shape changes modulate cell stiffness and cytoskeletal stresses. Consequently, topographic patterns might be used to induce specific cytoskeleton and nucleus stress states. To verify this, we performed whole cell force mapping with a spatial resolution of 1−2 μm, on cells cultivated on either patterned or flat pDR1m substrates. Additional experiments using glass slides or Petri dishes as support were performed to have reference values for cell stiffness and morphology on substrates, which are usually used in cell culture and mechanical measurements of cells. Force mapping allowed us to calculate the mechanical properties of different cellular regions by fitting the force−indentation curves with a Hertzian model, which has been widely used to characterize cell mechanics.[28,29] In normal conditions, for example cells cultivated on isotropic flat substrates, local elastic moduli can vary up to 2 orders of magnitude within the same cell, depending on the cell region (Figure 2A). Lower moduli were generally observed in the thicker areas of the cell, e.g. on the cell nuclear region. Conversely, the stiffest cell regions corresponded to thinner cell areas like lamellipodia or lamellae. Cells on the linear pattern are much more elongated and flattened (Figure 2B) in comparison to those observed on the flat substrate. Additionally, mechanical maps suggested that the average stiffness was higher on the patterned surface compared to the unpatterned case. In order to gain a better insight into the topography mediated cell morphology and local mechanical properties, we

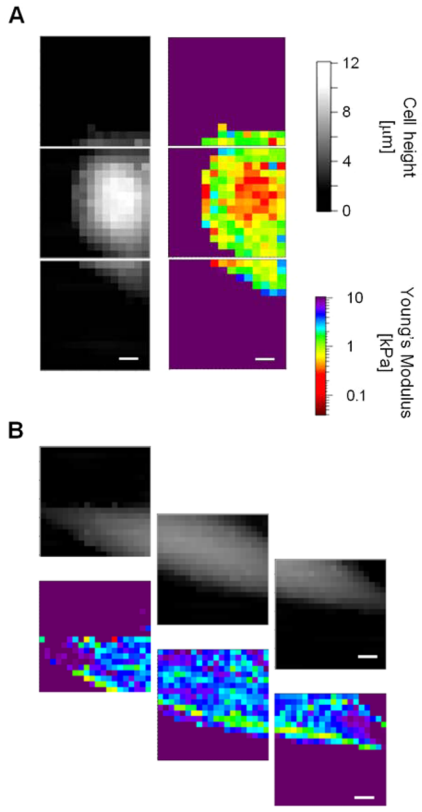

Figure 2. Height and elasticity maps of NIH-3T3 cells on (A) flat and (B) 2.5 μm pitch linear patterned pDR1m. Maps are 30 × 30 μm with pixels of 1.5 μm. Gray-scale map refers to cell heights, whereas color map refers to Young's modulus values. Scale bars are 5 μm.

first measured the stiffness as a function of cell thickness and compared corresponding values between different substrates.

We collected 1500−2000 force curves on cells for each substrate type, from which we extracted the elastic moduli and the contact point. By subtracting contact point values on cells and on substrates, we were able to calculate cell height values. The data of Young's modulus versus cell height are presented in Figure 3. Generally, we observed a softening of the modulus with increasing cell height. For very small cell thicknesses, when the indentation becomes a substantial fraction of the cell thickness, the assumption of the Hertz model used for analysis might not be valid anymore. In these cases the apparent Young's modulus will be much larger than the true value.[33,34] Thus, we excluded those force curves from further analysis, where the cell thickness was below 1 μm. Cell height alone can distinguish lamellipodial regions from the cell body; it can be assumed that the highest part of the cell is always in the nuclear area.[35] Thus we did not further label the different parts of the cells, but we used cell height values to discriminate different cell regions. An alternative way would have been to label selected cell components, such as the nucleus and the cytoskeleton with fluorescent vital stains. These, even if conventionally classified as vital, need to be translocated into the cytoplasm, for example with electroporation or lipofectants. However, this was reported to affect cell mechanical properties to a certain extent.[36] To discriminate the mechanical behavior of the different cell regions, we followed a more conservative approach. More specifically, we avoided the use of staining and considered the whole distribution cell heights. Moduli corresponding to the top 5% of heights were assumed to be representative of the

DOI: 10.1021/acsami.5b06693
ACS Appl. Mater. Interfaces 2015, 7, 21503−21510

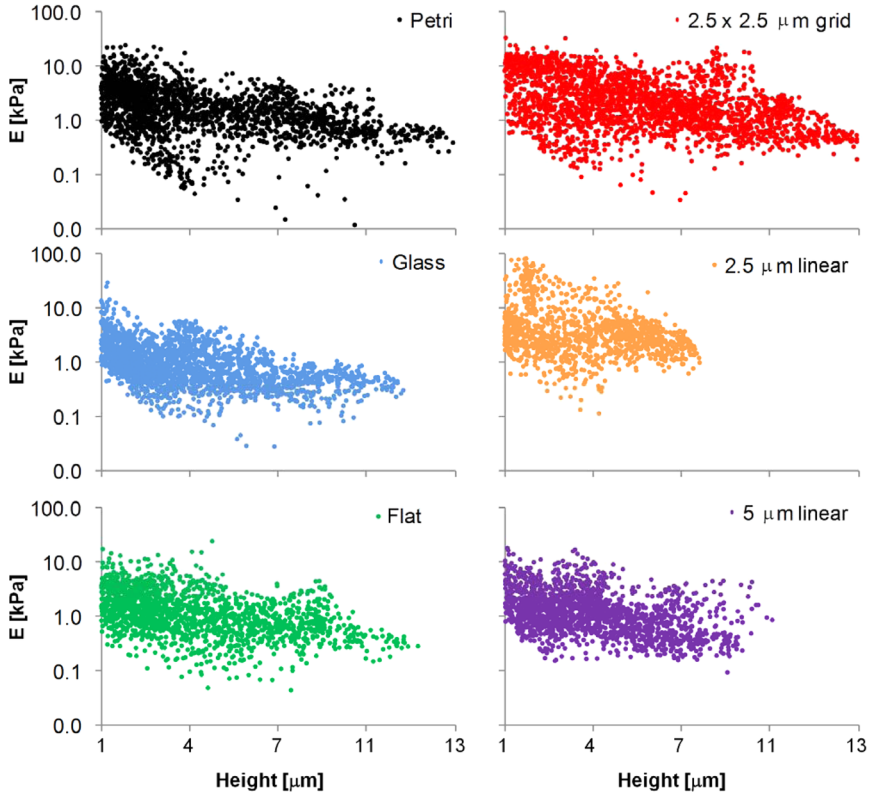

Figure 3. Semilog scatter plots of cell Young's modulus (E) versus cell height for the different substrates.

mechanical properties of the nuclear region. Conversely, we considered as elastic moduli of the cell body those calculated in a range centered in the median of all cell height values (corresponding to the range between the 40th and 60th percentiles).

According to this classification, we found that fibroblasts cultivated on patterned substrates possessed a significantly stiffer cell body with respect to those on flat surfaces. Furthermore, the highest values of elastic moduli were recorded on the 2.5 μm linear pattern, which were significantly higher than those measured on the 2.5 × 2.5 μm grid substrates and on the 5 μm patterns (Figure 4A). Similar results were observed for the moduli calculated in close proximity to the nuclear region: high values were measured in the case of the 2.5 μm linear pattern, whereas lower and similar moduli were observed on the 2.5 × 2.5 μm grid and the 5 μm linear pattern (Figure 4B).

We then investigated whether a dependency between cell body and nuclear stiffness existed. We found a positive dependency between the elastic moduli of the two cell regions, with the only exception of the cells cultivated on the 2.5 × 2.5 μm grid that displayed a relatively high cell body stiffness and an intermediate nuclear one (Figure 5).

The actin cytoskeleton plays a central role in determining mechanical properties of cells.[37,38] Additionally, actin bundles can deform the nucleus through the LINC complexes, thus possibly altering its mechanical response.[39,40] Therefore, we were interested in investigating whether surface patterning could affect cytoskeletal assemblies and if this may translate in alterations of nuclear shape and mechanics.

Cells on 2.5 μm linear patterns were highly elongated and the majority of stress fibers were located along the entire cell body length and were oriented along the pattern direction

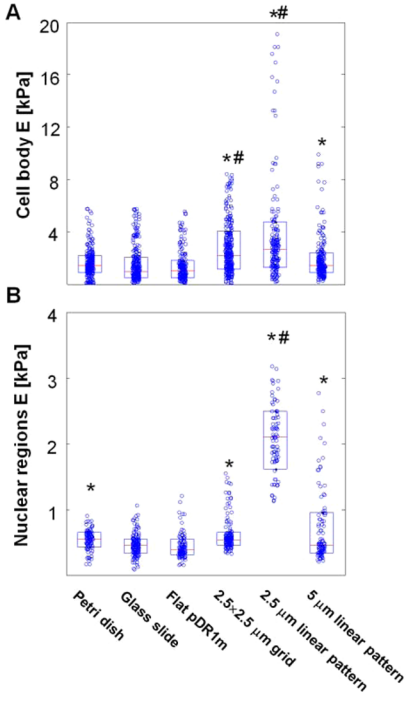

Figure 4. Box plots of the Young's modulus of (A) cell body and (B) nuclear regions of cells seeded on the different substrates. Blue boxes enclose the first and third quartiles, whereas the red mark is the median value. Blue open circles are the individual measurements. Number of data points in (A) (from left to right): 204; 238; 160, 239; 134; 180. Number of data points in (B) (from left to right): 82; 119; 80; 118; 59; 86. ∗ indicates significant differences with respect to the flat pDR1m substrate ($p < 0.05$); # indicates significant differences with respect to the 5 μm linear pattern ($p < 0.05$).

DOI: 10.1021/acsami.5b06693
ACS Appl. Mater. Interfaces 2015, 7, 21503−21510

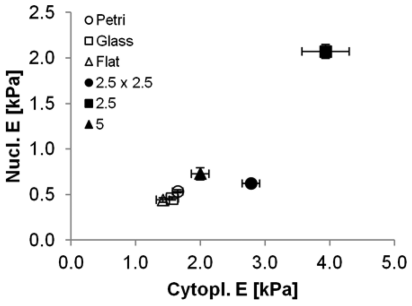

Figure 5. Scatter plot of the Young's modulus of the nuclear region (Nucl. E) versus cell body Young's modulus (Cytopl. E). Number of measurements is the same as in Figure 4. Bars are standard error of the mean.

(Figure 6A). Actin bundles were frequently seen in close contact with the nucleus and some fibers traced out nuclear

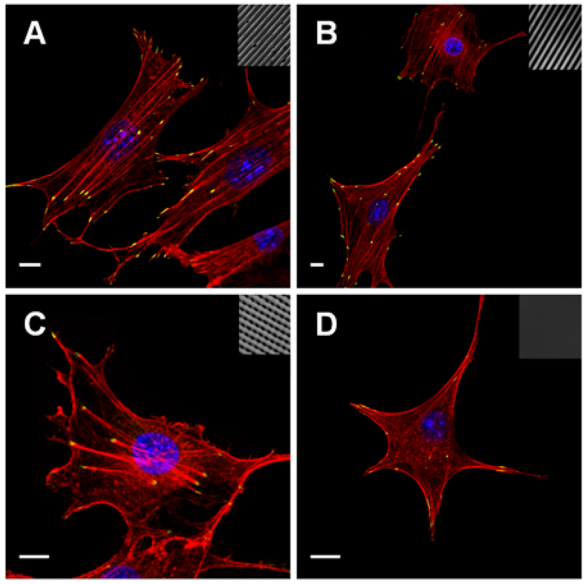

Figure 6. Confocal images of NIH-3T3 cell labeled with phalloidin (cytoskeleton), vinculin (focal adhesions), and To-Pro 3 (nuclei). Cells were cultivated on (A) 2.5 μm linear pattern, (B) 5 μm linear pattern, (C) 2.5 × 2.5 μm grid, and (D) flat pDR1m. Scale bars are 10 μm.

contours, suggesting an active squeezing of the nuclear envelope, which consequently appeared oblong in shape. Cells on the 5 μm linear pattern were less elongated and displayed a number of thick actin bundles far from the nucleus. In this case, the nucleus was also elliptical in shape, however, not as oblong as those on the 2.5 μm pattern (Figure 6B). Very different cytoskeleton structures formed in cells on the 2.5 × 2.5 μm grid pattern: a sparse network of thick and radially assembled fibers was observed (Figure 6C). Such a network was always located between the nucleus and the basal cell membrane. Lateral or apical stress fibers around the nucleus were almost absent, and as a consequence, the nucleus appeared spherical in shape. Cells on flat pDR1m substrates displayed a broad spectrum of morphologies ranging from spindle-like to circularly shaped cells (Figure 6D). Similarly, an actin cytoskeleton with aligned bundles was predominantly observed in spindle-like cells whereas a more isotropic network with randomly distributed fibers was seen in circular cells.

Owing to the diversity of the cytoskeletal assemblies on the substrates and the apparent shape of the nucleus, we asked whether a dependency between nuclear morphology and stiffness existed. Therefore, we evaluated the aspect ratio of the nuclear projected area and the nuclear volume; hence we plotted the Young's moduli of the nuclear regions versus these quantities. Nuclear regions with lower Young's moduli were observed in cells where nuclei had A/R values in the range 1.2–1.5 (Figure 7A). Even though cells on 5 μm patterns displayed

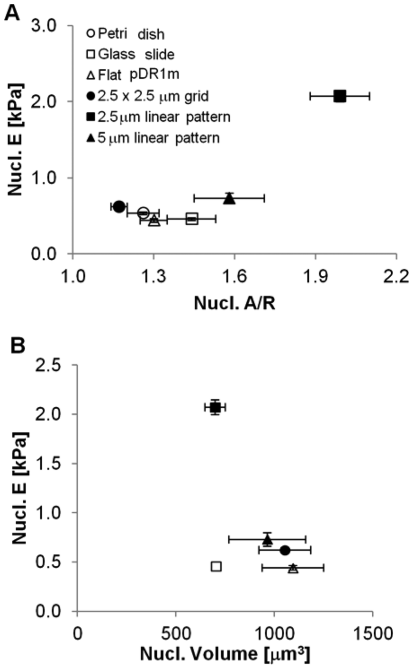

Figure 7. Scatter plots of the nuclear Young's modulus (Nucl. E) versus (A) nuclear A/R and (B) nuclear volume. Number of measurements for Nucl. E is the same as in Figure 4B. Number of measurements for nuclear A/R: Petri dish, 6; glass slide, 6; flat pDR1m, 6; 2.5 × 2.5 μm grid, 6; 2.5 μm linear, 12; 5 μm linear, 12. Number of measurements for nuclear volume: glass slide, 6; flat pDR1m, 6; 2.5 × 2.5 μm grid, 6; 2.5 μm linear, 12; 5 μm linear, 12. Bars represent standard error of the mean.

nuclei with a higher A/R value, nuclear stiffness was not significantly different from that measured in the case of cells on Petri dishes and on the 2.5 × 2.5 μm grid. Nuclei of cells cultivated on 2.5 μm linear patterns exhibited the highest value of A/R, although not significantly different from the one of cells on the 5 μm pattern, and the highest elastic modulus. Therefore, the A/R of the projected nuclear area does not correlate well with the mechanical properties of the nuclear region. Lateral compressive forces are not very effective in altering nuclear mechanical properties, probably because the nucleus can freely expand in the orthogonal direction. This prompted us to investigate the effects of the nuclear volume changes on the mechanical properties. With the exception of cells grown on glass slides, we found a much stronger dependence of the elastic modulus of the nuclear region on nuclear volume (Figure 7B). Highly elongated cells, such as those on the 2.5 μm pattern, possess oblong shape and smaller nuclei being also the stiffest. Closely packed acting bundles wrapping around the nuclear envelope are likely to exert substantial mechanical stress that ultimately compresses the nucleus. This is reasonable as the nuclear membrane is known

DOI: 10.1021/acsami.5b06693
ACS Appl. Mater. Interfaces 2015, 7, 21503–21510

to be porous and a volume reduction necessarily leads to a nuclear matter densification.[39] This determines an increase of the elastic modulus of the nuclear region. However, orderly arrays of contractile actin bundles, such as those observed in in the 2.5 μm pattern, might also contribute to the increased stiffness measured in the nuclear region. Larger nuclear volumes were observed in the case of cells having a cytoskeleton, at least partly, disconnected from the nucleus, as on the 2.5 × 2.5 μm grid and flat pDR1m substrates. In these cases, the cytoskeletal structure is not able to exert a coordinated nuclear compression and a subsequent volume reduction. Accordingly, the modulus of the nuclear region is low. An exception is presented by the nuclei of cells on bare glass. It is likely that surface mechanics or chemistry, more specifically different protein adsorption between pDR1m and glass, can affect nuclear mechanics besides topographic signals.[33,41] In particular, FA mediated signaling might alter the level of actomyosin contractility and hence the magnitude of the forces acting on the nuclear envelope.[42] Owing to the thickness of the plastic bottom of the Petri dishes, *z*-stack images acquired with the high magnification objective lenses were extensively blurred. Therefore, we were not able to measure nuclear volume of cells cultivated on Petri dishes accurately.

Cell mechanics is strongly affected by environmental cues. In particular, the physical/mechanical characteristics of the supporting material are known to exert a potent effect on cell stiffness. Several studies were focused in elucidating the effect of the substrate properties on cell stiffness using various techniques.[15−18] Generally, more rigid materials provoke cells to become stiffer, whereas soft materials, such as hydrogels, make cells more compliant.[19,20] These findings are of particular interest not only in diagnostics as altered cellular mechanical properties might underlie a pathological state, but also in regenerative medicine since the transduction of exogenous mechanical signals can ultimately dictate cell fate and functions.[6,43,44] Despite such detailed knowledge on material stiffness and mechanotransduction, the effects of surface topography on cell mechanics have been, in comparison, scarcely investigated.

AFM has been widely used to investigate cell mechanical properties.[45] Relevant mechanical parameters describing a cell's elasticity/viscoelasticity were found to correlate with specific cell states such as differentiation, aging, and disease.[46−49] By selectively disrupting cytoskeleton components, AFM studies revealed that cell stiffness is predominantly dictated by the actin network. Since topographic patterns profoundly affect actin cytoskeleton assembly and dynamics,[21] it is expected that these patterns also have an impact on cell mechanics. Encoding topographic patterns on materials surfaces can be performed in various manners. In the case of micrometer-scale patterns, soft lithography is one of the most used techniques.[50] In this work, however, we used azopolymer substrates since topographic features can be easily created on them without the use of specifically dedicated apparatus. Furthermore, azopolymers were successfully employed for cell culture experiments with no additional surface functionalization. The Hurduc group developed a range of azo-polysiloxanes as biocompatible substrates.[51,52] They addressed the importance of polymer stability in aqueous environment as a crucial factor in affecting cell adhesion and morphology. By using an azo-based methacrylic chromophoric terpolymer, Barillé et al.[53] created micro- and nanogratings that significantly affected neuron polarization and neurite outgrowth in vitro. Additionally, they also reported good proliferation rates, demonstrating that azopolymers are useful to affect various aspects of cell behavior in vitro.

By combining topographic patterns and AFM measurements, Hansen et al.[41] studied the elasticity of MC3T3-E1 cells on flat and nanostructured polymeric substrates. They found that cells on the nanoscale topographical features were stiffer than those cultivated on flat control substrates. Similarly, McPhee et al.[11] reported that NIH-3T3 fibroblasts displayed higher mechanical properties on microgrooved elastomeric substrates with respect to cells cultivated on flat controls. More recently, McKee et al.[54] found that the geometrical features of patterned substrates affect both nuclear shape and modulus. They hypothesized that the nucleus could directly act as a mechanosensor of the substrate topography, whose signals can influence cell alignment and proliferation. Topographic patterns also proved to induce epigenetic changes in differentiated cells. In fact, Downing et al.[55] demonstrated that micrometric gratings profoundly affected cell and nuclear shape that were sufficient to modulate both acetylation and methylation of histones involved in cell reprogramming. Our results provide further evidence of the role of topographic signals in affecting nuclear shape and mechanics. Confocal micrographs revealed diverse cytoskeletal structures that formed on the topographies, and these structures interacted differently with the nucleus, highlighting how cytoskeletal assemblies and cell body mechanics appear regulated by the underlying micropattern. In fact, actin bundles are connected to the nuclear envelope with specific linkers and therefore changes in the cytoskeletal structures can be directly transferred to the nucleus. Additionally, actomyosin generated forces can stand on the nuclear envelope thus altering its structure dynamically. Versaevel et al.[39] found that lateral compressive forces generated by actin bundles regulated nuclear orientation and deformation. Cells cultivated on micropatterned adhesive islands developed anisotropic contraction dipoles that altered nuclear shape and induced chromatin condensation. In our experiments, micro-topography acts at the level of FAs by confining their formation and guiding their growth. As we have recently reported,[32] in the case of narrow ridges, such as in 2.5 μm patterns, FAs forming orthogonal to the pattern direction are unstable and more prone to collapse upon actin contraction. Such a collapse not only causes the cytoskeleton to be coaligned with the pattern, but also causes the cell to acquire a narrow spindle-like morphology with a highly elongated nucleus (Figures 6A and 7A). Furthermore, the coordinated contraction exerted by the actin cytoskeleton all around the nucleus causes a significant volume decrease (Figure 7B). Altogether, shape and volume changes can be responsible for nuclear matter densification and hence an increase of the measured stiffness on nuclear regions. Larger features, and more specifically larger ridges such as in the 5 μm linear patterns, enable the FAs to grow to significant lengths even in directions orthogonal to that of the pattern. In this case, cells can acquire a more spread morphology with a cytoskeleton that is distributed all over the cell body (Figure 6B). Here, the nucleus is less stressed with respect to what is found in the 2.5 μm pattern case, and takes on a less compressed shape (Figure 7). Accordingly, elastic moduli on nuclear regions were lower. A very peculiar response of the NIH-3T3 to the 2.5 × 2.5 μm grid was observed. Such a substrate allowed FAs to establish only on a limited area, and their maturation was inhibited by the small size of the topographic features. Cells usually displayed ragged edges,

DOI: 10.1021/acsami.5b06693
ACS Appl. Mater. Interfaces 2015, 7, 21503−21510

and the cytoskeleton was constituted by few bundles arranged in a star-shaped manner (Figure 6C). This structure formed between the pattern and the nucleus. The nuclear envelope was apparently disengaged from the actin cytoskeleton as the nucleus was thicker (Figure 3), rounder (Figure 7A), and more compliant (Figure 4B). Furthermore, the use of azopolymers might in principle allow analyzing topography mediated mechanotransduction in a dynamic environment. In fact, as topographic signals in vivo change in time and space owing to active cellular remodeling or to deformation arising from external forces, light-sensitive surfaces represent a reliable tool that is able to display topographic signals whose features can be modulated dynamically, thus capturing the unique characteristics of the in vivo microenvironment.

We believe that taken together these data represent strong evidence of the fact that topographic patterns are very effective in modulating the material−cytoskeleton crosstalk. Patterns regulate cytoskeleton assembly and hence nuclear shape along with the forces acting on the nuclear envelope. This notwithstanding, additional investigations at the biomolecular level may support these observations. Finally, these results can in principle be used to design topographic patterns able to transfer mechanical information up to the nucleus, thus influencing cell fate and functions.

4. CONCLUSIONS

In this work we showed that micropatterned azopolymer substrates strongly influence cell mechanical properties of the cell body and nuclear regions along with cytoskeleton assembly and nuclei morphology. In particular, we found that cells on linear patterns were elongated, possessing a highly structured cytoskeleton and characterized by smaller nuclei with respect to flat substrates and grid pattern (nucleus volume of about 700 μm^3 on 2.5 μm linear pattern and 1100 μm^3 on flat substrates). Correspondingly, elastic modulus values on cell body and nuclear regions were higher and cells were thinner on micropatterned azopolymers with respect to flat samples (nuclear regions were characterized by elastic moduli up to 2 kPa on 2.5 μm linear pattern and 400 Pa on flat sample; cells were of about 7 μm height on 2.5 μm linear pattern and up to 12 μm on flat samples). Furthermore, a dependency between mechanical proprieties of cell nuclear regions and nuclei morphology was found. In fact, highly elongated cells possessed oblong shape and smaller nuclei being also the stiffest ones.

These results demonstrate that the use of azopolymers as cell culture supports may pave the way to the study of cell mechanics in a dynamic and biomimetic way, owing to unique properties of the azobenzene moieties that are able to change their conformation in response to light stimuli. This result may become useful in the development of new "cell-instructive" biomaterials for tissue engineering.

AUTHOR INFORMATION

Corresponding Author

*E-mail: nettipa@unina.it.

Present Address

C.R.: Institute of Biophysics, University of Bremen, Otto-Hahn Allee, D-28359 Bremen, Germany.

Notes

The authors declare no competing financial interest.

ACKNOWLEDGMENTS

The authors thank Prof. P. Ferraro, Dr. V. Pagliarulo, and Mr. A. Calabuig for providing the Lloyd's mirror setup; Mr. H. Doschke for the technical support in AFM data analysis; Dr. C. Natale for his suggestions in cell cultures and staining procedures; and Ms. V. La Tilla for drawing the table of content graphics. The authors acknowledge COST Action TD1002 AFM4NanoMed&Bio (COST-STSM-TD1002-18687) for providing the financial support during the scientific term in Bremen.

REFERENCES

(1) Lutolf, M.; Hubbell, J. Synthetic Biomaterials as Instructive Extracellular Microenvironments for Morphogenesis in Tissue Engineering. *Nat. Biotechnol.* **2005**, *23*, 47−55.

(2) Sengupta, D.; Waldman, S. D.; Li, S. From in Vitro to in Situ Tissue Engineering. *Ann. Biomed. Eng.* **2014**, *42*, 1537−1545.

(3) Yeung, T.; Georges, P. C.; Flanagan, L. A.; Marg, B.; Ortiz, M.; Funaki, M.; Zahir, N.; Ming, W.; Weaver, V.; Janmey, P. A. Effects of Substrate Stiffness on Cell Morphology, Cytoskeletal Structure, and Adhesion. *Cell Motil. Cytoskeleton* **2005**, *60*, 24−34.

(4) Van Kooten, T. G.; Spijker, H. T.; Busscher, H. J. Plasma-Treated Polystyrene Surfaces: Model Surfaces for Studying Cell−Biomaterial Interactions. *Biomaterials* **2004**, *25*, 1735−1747.

(5) Flemming, R.; Murphy, C.; Abrams, G.; Goodman, S.; Nealey, P. Effects of Synthetic Micro- and Nano-Structured Surfaces on Cell Behavior. *Biomaterials* **1999**, *20*, 573−588.

(6) Engler, A. J.; Sen, S.; Sweeney, H. L.; Discher, D. E. Matrix Elasticity Directs Stem Cell Lineage Specification. *Cell* **2006**, *126*, 677−689.

(7) Kilian, K. A.; Bugarija, B.; Lahn, B. T.; Mrksich, M. Geometric Cues for Directing the Differentiation of Mesenchymal Stem Cells. *Proc. Natl. Acad. Sci. U. S. A.* **2010**, *107*, 4872−4877.

(8) Dalby, M. J.; Gadegaard, N.; Tare, R.; Andar, A.; Riehle, M. O.; Herzyk, P.; Wilkinson, C. D. W.; Oreffo, R. O. C. The Control of Human Mesenchymal Cell Differentiation Using Nanoscale Symmetry and Disorder. *Nat. Mater.* **2007**, *6*, 997−1003.

(9) McNamara, L. E.; McMurray, R. J.; Biggs, M. J.; Kantawong, F.; Oreffo, R. O.; Dalby, M. J. Nanotopographical Control of Stem Cell Differentiation. *J. Tissue Eng.* **2010**, *1*, 120623.

(10) González-Cruz, R. D.; Fonseca, V. C.; Darling, E. M. Cellular Mechanical Properties Reflect the Differentiation Potential of Adipose-Derived Mesenchymal Stem Cells. *Proc. Natl. Acad. Sci. U. S. A.* **2012**, *109*, E1523−E1529.

(11) McPhee, G.; Dalby, M. J.; Riehle, M.; Yin, H. Can Common Adhesion Molecules and Microtopography Affect Cellular Elasticity? A Combined Atomic Force Microscopy and Optical Study. *Med. Biol. Eng. Comput.* **2010**, *48*, 1043−1053.

(12) Khani, M.-M.; Tafazzoli-Shadpour, M.; Rostami, M.; Peirovi, H.; Janmaleki, M. Evaluation of Mechanical Properties of Human Mesenchymal Stem Cells During Differentiation to Smooth Muscle Cells. *Ann. Biomed. Eng.* **2014**, *42*, 1373−1380.

(13) Lekka, M.; Laidler, P.; Gil, D.; Lekki, J.; Stachura, Z.; Hrynkiewicz, A. Elasticity of Normal and Cancerous Human Bladder Cells Studied by Scanning Force Microscopy. *Eur. Biophys. J.* **1999**, *28*, 312−316.

(14) Prabhune, M.; Belge, G.; Dotzauer, A.; Bullerdiek, J.; Radmacher, M. Comparison of Mechanical Properties of Normal and Malignant Thyroid Cells. *Micron* **2012**, *43*, 1267−1272.

(15) Hochmuth, R. M. Micropipette Aspiration of Living Cells. *J. Biomech.* **2000**, *33*, 15−22.

(16) Zhang, H.; Liu, K.-K. Optical Tweezers for Single Cells. *J. R. Soc., Interface* **2008**, *5*, 671−690.

(17) Laurent, V. M.; Hénon, S.; Planus, E.; Fodil, R.; Balland, M.; Isabey, D.; Gallet, F. Assessment of Mechanical Properties of Adherent Living Cells by Bead Micromanipulation: Comparison of Magnetic

DOI: 10.1021/acsami.5b06693
ACS Appl. Mater. Interfaces 2015, 7, 21503−21510

Twisting Cytometry vs Optical Tweezers. *J. Biomech. Eng.* **2002**, *124*, 408−421.
(18) Radmacher, M. Measuring the Elastic Properties of Biological Samples with the AFM. *Eng. Med. Biol. Mag. IEEE* **1997**, *16*, 47−57.
(19) Sunyer, R.; Jin, A. J.; Nossal, R.; Sackett, D. L. Fabrication of Hydrogels with Steep Stiffness Gradients for Studying Cell Mechanical Response. *PLoS One* **2012**, *7*, e46107.
(20) Thomas, G.; Burnham, N. A.; Camesano, T. A.; Wen, Q. Measuring the Mechanical Properties of Living Cells Using Atomic Force Microscopy. *J. Visualized Exp.* **2013**, *76*, e50497.
(21) Natale, C. F.; Ventre, M.; Netti, P. A. Tuning the Material-Cytoskeleton Crosstalk Via Nanoconfinement of Focal Adhesions. *Biomaterials* **2014**, *35*, 2743−2751.
(22) Ramdas, N. M.; Shivashankar, G. Cytoskeletal Control of Nuclear Morphology and Chromatin Organization. *J. Mol. Biol.* **2015**, *427*, 695−706.
(23) Rochon, P.; Batalla, E.; Natansohn, A. Optically Induced Surface Gratings on Azoaromatic Polymer Films. *Appl. Phys. Lett.* **1995**, *66*, 136−138.
(24) Kim, D.; Tripathy, S.; Li, L.; Kumar, J. Laser-Induced Holographic Surface Relief Gratings on Nonlinear Optical Polymer Films. *Appl. Phys. Lett.* **1995**, *66*, 1166−1168.
(25) Bian, S.; Li, L.; Kumar, J.; Kim, D.; Williams, J.; Tripathy, S. Single Laser Beam-Induced Surface Deformation on Azobenzene Polymer Films. *Appl. Phys. Lett.* **1998**, *73*, 1817−1819.
(26) Ambrosio, A.; Camposeo, A.; Carella, A.; Borbone, F.; Pisignano, D.; Roviello, A.; Maddalena, P. Realization of Submicrometer Structures by a Confocal System on Azopolymer Films Containing Photoluminescent Chromophores. *J. Appl. Phys.* **2010**, *107*, 083110.
(27) Hutter, J. L.; Bechhoefer, J. Calibration of Atomic-Force Microscope Tips. *Rev. Sci. Instrum.* **1993**, *64*, 1868−1873.
(28) Hertz, H. Über die Berührung Fester Elastischer Körper. *J. Reine Angew. Math.* **1882**, *92*, 156−171.
(29) Radmacher, M. In *Atomic Force Microscopy in Cell Biology*; Jena, B. P., Hörber, J. K. H., Eds.; Elsevier: Amsterdam, 2002; Chapter 4, pp 67−87.
(30) Schindelin, J.; Arganda-Carreras, I.; Frise, E.; Kaynig, V.; Longair, M.; Pietzsch, T.; Preibisch, S.; Rueden, C.; Saalfeld, S.; Schmid, B.; Tinevez, J.-Y.; White, D. J.; Hartenstein, V.; Eliceiri, K.; Tomancak, P.; Cardona, A. Fiji: An Open-Source Platform for Biological-Image Analysis. *Nat. Methods* **2012**, *9*, 676−682.
(31) Rianna, C.; Calabuig, A.; Ventre, M.; Cavalli, S.; Pagliarulo, V.; Grilli, S.; Ferraro, P.; Netti, P. A. Reversible Holographic Patterns on Azopolymers for Guiding Cell Adhesion and Orientation. *ACS Appl. Mater. Interfaces* **2015**, *7*, 16984−16991.
(32) Ventre, M.; Natale, C. F.; Rianna, C.; Netti, P. A. Topographic Cell Instructive Patterns to Control Cell Adhesion, Polarization and Migration. *J. R. Soc., Interface* **2014**, *11*, 20140687.
(33) Domke, J.; Dannöhl, S.; Parak, W. J.; Müller, O.; Aicher, W. K.; Radmacher, M. Substrate Dependent Differences in Morphology and Elasticity of Living Osteoblasts Investigated by Atomic Force Microscopy. *Colloids Surf., B* **2000**, *19*, 367−379.
(34) Gavara, N.; Chadwick, R. S. Determination of the Elastic Moduli of Thin Samples and Adherent Cells Using Conical Atomic Force Microscope Tips. *Nat. Nanotechnol.* **2012**, *7*, 733−736.
(35) Rheinlaender, J.; Schäffer, T. E. Mapping the Mechanical Stiffness of Live Cells with the Scanning Ion Conductance Microscope. *Soft Matter* **2013**, *9*, 3230−3236.
(36) Fuhrmann, A.; Staunton, J.; Nandakumar, V.; Banyai, N.; Davies, P.; Ros, R. AFM Stiffness Nanotomography of Normal, Metaplastic and Dysplastic Human Esophageal Cells. *Phys. Biol.* **2011**, *8*, 015007.
(37) Moeendarbary, E.; Valon, L.; Fritzsche, M.; Harris, A. R.; Moulding, D. A.; Thrasher, A. J.; Stride, E.; Mahadevan, L.; Charras, G. T. The Cytoplasm of Living Cells Behaves as a Poroelastic Material. *Nat. Mater.* **2013**, *12*, 253−261.
(38) Rotsch, C.; Radmacher, M. Drug-Induced Changes of Cytoskeletal Structure and Mechanics in Fibroblasts: An Atomic Force Microscopy Study. *Biophys. J.* **2000**, *78*, 520−535.
(39) Versaevel, M.; Grevesse, T.; Gabriele, S. Spatial Coordination Between Cell and Nuclear Shape Within Micropatterned Endothelial Cells. *Nat. Commun.* **2012**, *3*, 671.
(40) Dahl, K. N.; Ribeiro, A. J.; Lammerding, J. Nuclear Shape, Mechanics, and Mechanotransduction. *Circ. Res.* **2008**, *102*, 1307−1318.
(41) Hansen, J. C.; Yul Lim, J.; Xu, L.-C.; Siedlecki, C. A.; Mauger, D. T.; Donahue, H. J. Effect of Surface Nanoscale Topography on Elastic Modulus of Individual Osteoblastic Cells as Determined by Atomic Force Microscopy. *J. Biomech.* **2007**, *40*, 2865−2871.
(42) Dalby, M. J.; Gadegaard, N.; Oreffo, R. O. C. Harnessing Nanotopography and Integrin−Matrix Interactions to Influence Stem Cell Fate. *Nat. Mater.* **2014**, *13*, 558−569.
(43) Denais, C.; Lammerding, J. In *Cancer Biology and the Nuclear Envelope*; Schirmer, E. C., De Las Heras, J. I., Eds.; Springer: New York, 2014; Chapter 21, pp 435−470.
(44) Swift, J.; Ivanovska, I. L.; Buxboim, A.; Harada, T.; Dingal, P. D. P.; Pinter, J.; Pajerowski, J. D.; Spinler, K. R.; Shin, J.-W.; Tewari, M.; Rehfeldt, F.; Speicher, D. W.; Discher, D. E. Nuclear Lamin-A Scales with Tissue Stiffness and Enhances Matrix-Directed Differentiation. *Science* **2013**, *341*, 1240104.
(45) Haase, K.; Pelling, A. E. Investigating Cell Mechanics with Atomic Force Microscopy. *J. R. Soc., Interface* **2015**, *12*, 20140970.
(46) González-Cruz, R. D.; Fonseca, V. C.; Darling, E. M. Cellular Mechanical Properties Reflect the Differentiation Potential of Adipose-Derived Mesenchymal Stem Cells. *Proc. Natl. Acad. Sci. U. S. A.* **2012**, *109*, E1523−E1529.
(47) Lieber, S. C.; Aubry, N.; Pain, J.; Diaz, G.; Kim, S. J.; Vatner, S. F. Aging Increases Stiffness of Cardiac Myocytes Measured by Atomic Force Microscopy Nanoindentation. *Am. J. Physiol. Heart Circ. Physiol.* **2004**, *287*, H645−H651.
(48) Berdyyeva, T. K.; Woodworth, C. D.; Sokolov, I. Human Epithelial Cells Increase Their Rigidity with Ageing in Vitro: Direct Measurements. *Phys. Med. Biol.* **2005**, *50*, 81−92.
(49) Cross, S. E.; Jin, Y. S.; Rao, J.; Gimzewski, J. K. Nanomechanical Analysis of Cells from Cancer Patients. *Nat. Nanotechnol.* **2007**, *2*, 780−783.
(50) Yao, X.; Peng, R.; Ding, J. Cell-Material Interactions Revealed Via Material Techniques of Surface Patterning. *Adv. Mater.* **2013**, *25*, 5257−5286.
(51) Hurduc, N.; Macovei, A.; Paius, C.; Raicu, A.; Moleavin, I.; Branza-Nichita, N.; Hamel, M.; Rocha, L. Azo-polysiloxanes as New Supports for Cell Cultures. *Mater. Sci. Eng., C* **2013**, *33*, 2440−2445.
(52) Rocha, L.; Păiuş, C.-M.; Luca-Raicu, A.; Resmerita, E.; Rusu, A.; Moleavin, I.-A.; Hamel, M.; Branza-Nichita, N.; Hurduc, N. Azobenzene Based Polymers as Photoactive Supports and Micellar Structures for Applications in Biology. *J. Photochem. Photobiol., A* **2014**, *291*, 16−25.
(53) Barillé, R.; Janik, R.; Kucharski, S.; Eyer, J.; Letournel, F. Photo-Responsive Polymer with Erasable and Reconfigurable Micro- and Nano-Patterns: An in Vitro Study for Neuron Guidance. *Colloids Surf., B* **2011**, *88*, 63−71.
(54) McKee, C. T.; Raghunathan, V. K.; Nealey, P. F.; Russell, P.; Murphy, C. J. Topographic Modulation of the Orientation and Shape of Cell Nuclei and Their Influence on the Measured Elastic Modulus of Epithelial Cells. *Biophys. J.* **2011**, *101*, 2139−2146.
(55) Downing, T. L.; Soto, J.; Morez, C.; Houssin, T.; Fritz, A.; Yuan, F.; Chu, J.; Patel, S.; Schaffer, D. V.; Li, S. Biophysical Regulation of Epigenetic State and Cell Reprogramming. *Nat. Mater.* **2013**, *12*, 1154−1162.

DOI: 10.1021/acsami.5b06693
ACS Appl. Mater. Interfaces 2015, 7, 21503−21510